

Adaptive Passivity Based Control of DC-DC Power Electronic Converters

Anushka M. Dissanayake and Nishantha C. Ekneligoda

School of Electrical and Computer Engineering

Oklahoma State University

Stillwater, OK 74078, USA

Email: anushkd@okstate.edu, nishantha.ekneligoda@okstate.edu

Abstract—Application of power electronic converters and their controls play a vital role in modern industry. Advanced nonlinear controls with adaptation are required to control these converters when all or some of the system parameters are unknown or uncertain. Design of a passivity based nonlinear adaptive controller to control the output voltage of power electronic converter is proposed in this paper. Unlike most of the other adaptive controllers which require the input voltage information of the converter, the proposed controller require neither input voltage information nor output load resistance. Taking the duty cycle as the control input of the boost converter, the adaptive passivity based controller is designed to regulate the output voltage of the converter to a desired value. However, the proposed approach can be easily extended to control any other DC-DC converter without loss of generality. Simulation and experimental verifications were carried out to analyze the performance and the effectiveness of the proposed controller.

I. INTRODUCTION

Power electronics (PEs) and their controls have gained more attention in recent years due to the development in smart power grids, improved electric drive systems and electric vehicles [1]–[3]. Among the PE converter control methods, most popular choice of the control algorithm is the PI control approach. Even though, it is the most simple and easiest algorithm, it has very poor transient performances [4]. Hence an advance control algorithms are required to replace the PI control loops in PE converter domain.

Novel control methodologies based on nonlinear control architecture, predictive control, optimal and game theoretic control have been proposed to stabilize PE converters [5]–[9]. In order to regulate the output voltage of boost and buck converters, a nonlinear controller is proposed in [5]. In order to provide an additional tuning parameter to modify the output response, the developed controller assumes the exponential form of the linear multiloop controller. A design of a closed loop control of DC-DC buck converters based on the exact feedback linearization is presented in [6]. Here, the precise model of the dynamical system including the parasitic resistances of the inductor, capacitor and switches together with the averaged state space method is used to develop the controller. Optimal control is applied in [7] to control the DC-DC converters in a microgrid. Here, optimal voltage and power regulation of the converters are formulated for distributed generators in DC microgrids. Game theoretic control of DC-DC converters in energy and impedance domain are discussed in [8] and [9].

Open loop optimal control trajectories of the converters are obtained in [8] using the Pontryagin's minimum principle. In contrast, an online feedback strategy is proposed in [9] to control the PE converters. A reduced order observer based output feedback controller is designed in [10] for DC-DC buck power converter. In this approach, authors assumed that current information is unavailable and then a state feedback controller is designed with the estimated state information.

In closed loop feedback control of PE converters, usually it requires the knowledge of complete dynamical system and its parameters to develop a controller [11]. When a PE converter has parameter uncertainties or when the complete converter dynamics are unavailable, adaptive controllers are required to control the converter [12]. Adaptive controls applied in PE converters can be found in [13]–[19]. Among them, work presented in [13]–[15] demonstrate adaptive control strategies developed for buck power converter. A neural network based adaptive decentralized controller for the buck converter is proposed in [13]. In this modeling, the buck converter behaves as the interface between a PV array and a microgrid. Dynamic model of the converter is obtained in feedback linearizable form and the neural network universal approximation property is used to approximate the unknown dynamics of the system when developing the control algorithm. An application of the adaptive backstepping nonlinear control methodology in buck converter is presented in [14]. In this work a Chebyshev neural network based technique is formulated to regulate the output voltage under load uncertainties. Considering both unknown input voltage and output load an adaptive, finite time controller for voltage regulation in buck converter is proposed in [15]. In this approach two finite-time convergent observers are designed in the controller to estimate the unknown parameters in a finite time.

Adaptive feedback controllers developed to control boost PE converters can be found in [16]–[19]. Motivated by the passive nature of the DC-DC power converters, passivity based adaptive controllers are designed for the boost and buck-boost converters in [16]. An adaptive pulse width modulation (PWM) strategy has been proposed in [17] based on the sliding mode control (SMC) to regulate the output voltage of a boost converter. An adaptive feed forward compensation technique is proposed in [18] for the boost power converter to address the uncertainty issues in the system dynamics. In [19], an adaptive

fuzzy neural control methodology is developed for the voltage tracking of the boost power converter while improving the robustness of the converter during the transient stage, through a total sliding mode control.

Most of the adaptive strategies developed in the literature require input voltage information of the converter. This paper proposes a methodology to eliminates this constraint by introducing an adaptive feedback controller based on the passivity architecture. Hence, the proposed controller neither require input voltage information nor the output load resistance to regulate the output voltage. Boost DC-DC power converter is used to demonstrate the proposed concept which can be easily extend to other types of DC-DC PE converters.

The rest of the paper is organized as follows. In section II, mathematical modeling of the boost power converter and the proposed controller is derived. Simulation and experimental verifications are given in sections III and IV respectively. Finally the paper is concluded in section V.

II. MATHEMATICAL MODELING

Mathematical modeling of the boost PE converter and adaptive passivity controller is given in this section. The schematic model of the boost converter can be shown as in Fig. 1. The average model of this boost converter [11] in the continuous conduction mode [20] is mathematically presented in (1) and (2).

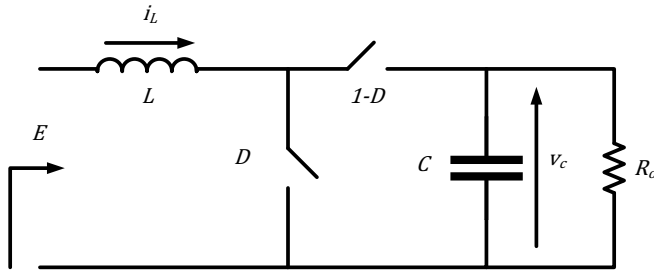


Fig. 1. Schematic diagram of DC-DC boost power converter.

$$\dot{x}_1 = \frac{1}{L}[-(1-u)x_2 + E] \quad (1)$$

$$\dot{x}_2 = \frac{1}{C}[(1-u)x_1 - \theta x_2] \quad (2)$$

where, the two states $x_1 = i_L$, $x_2 = v_c$ are the inductor current and capacitor voltage, control input u is the duty cycle D , and L, C, E, θ are the inductance of the inductor, capacitance of the capacitor, input voltage and conductance of the output load resistance ($\theta = 1/R_o$). Define the state vector as $x = [x_1 \ x_2]^T$, unknown constant parameter vector in the system as $\Theta = [E \ \theta]^T$ and the parameter estimate vector of the unknowns as $\hat{\Theta} = [\hat{E} \ \hat{\theta}]^T$. The system given in (1) and (2) with the estimates of the input voltage and output load resistance can be represented as,

$$\mathcal{D}\dot{x} + (1-u)\mathcal{J}x + \mathcal{R}x = \xi \quad (3)$$

where, $\mathcal{D} = \begin{bmatrix} L & 0 \\ 0 & C \end{bmatrix}$, $\mathcal{J} = \begin{bmatrix} 0 & 1 \\ -1 & 0 \end{bmatrix}$, $\mathcal{R} = \begin{bmatrix} 0 & 0 \\ 0 & \hat{\theta} \end{bmatrix}$, $\xi = \begin{bmatrix} \hat{E} \\ 0 \end{bmatrix}$. The goal of the controller is to regulate output voltage (x_2) to the desired constant value (V_d). Indirect control is used because of the non-minimum phase behavior of the boost converter [11]. Therefore, the output voltage regulation problem becomes a regulation problem of the inductor current (x_1) to its corresponding constant desired value ($x_{1d} = V_d^2 \hat{\theta} / \hat{E}$). Hence, the desired state vector will be $x_d = \begin{bmatrix} x_{1d} \\ x_{2d} \end{bmatrix}$. Next, the error states are defined as $\tilde{x}_1 = x_1 - x_{1d}$, $\tilde{x}_2 = x_2 - x_{2d}$ and the error vector is defined as $\tilde{x} = \begin{bmatrix} \tilde{x}_1 \\ \tilde{x}_2 \end{bmatrix}$. Then, the error dynamics can be presented as,

$$\mathcal{D}\dot{\tilde{x}} + (1-u)\mathcal{J}\tilde{x} + \mathcal{R}\tilde{x} = \xi - (\mathcal{D}\dot{x}_d + (1-u)\mathcal{J}x_d + \mathcal{R}x_d) \quad (4)$$

By adding a damping (dissipation term) to both sides of (4), the error dynamics can be remodeled as [16],

$$\mathcal{D}\dot{\tilde{x}} + (1-u)\mathcal{J}\tilde{x} + \mathcal{R}_d\tilde{x} = \Psi \quad (5)$$

$$\Psi = \xi - (\mathcal{D}\dot{x}_d + (1-u)\mathcal{J}x_d + \mathcal{R}x_d - \mathcal{R}_I\tilde{x}) \quad (6)$$

where, $\mathcal{R}_I = \begin{bmatrix} \mathcal{R}_1 & 0 \\ 0 & 0 \end{bmatrix}$, $\mathcal{R}_1 > 0$, and $\mathcal{R}_d = \mathcal{R}_I + \mathcal{R}$. Suppose Ψ is replaced by a known matrix \mathcal{Y} and the estimation error vector $\tilde{\Theta} = \hat{\Theta} - \Theta = \begin{bmatrix} \tilde{E} \\ \tilde{\theta} \end{bmatrix}$. Then, the error dynamics take the form,

$$\mathcal{D}\dot{\tilde{x}} + (1-u)\mathcal{J}\tilde{x} + \mathcal{R}_d\tilde{x} = \mathcal{Y}\tilde{\Theta} \quad (7)$$

where, $\mathcal{Y} = \begin{bmatrix} -1 & 0 \\ 0 & x_{2d} \end{bmatrix}$. Now the system under consideration is $\begin{bmatrix} \tilde{x} \\ \tilde{\Theta} \end{bmatrix} \in \mathbb{R}^4$. Considering the energy based quadratic, positive definite, radially unbounded Lyapunov candidate given in (8).

$$\mathcal{H} = \frac{1}{2}[\tilde{x}^T \mathcal{D}\tilde{x} + \tilde{\Theta}^T \Gamma^{-1}\tilde{\Theta}] \quad (8)$$

where, $\Gamma = \begin{bmatrix} \Gamma_1 & 0 \\ 0 & \Gamma_2 \end{bmatrix}$, $\Gamma_1, \Gamma_2 > 0$ is the gain matrix which can be used to adjust the parameter convergence rates. Taking the time derivative of (8) along the dynamics given by (7), adaptation law for the estimates can be derived as (9). This adaptive law makes the Lyapunov candidate derivative negative ($\dot{\mathcal{H}} < 0$).

$$\dot{\hat{\Theta}} = -\Gamma(\mathcal{Y}\tilde{x} - \sigma\hat{\Theta}) \quad (9)$$

where, $\sigma > 0$ is a constant design parameter. In order to satisfy the condition $\Psi = \mathcal{Y}\tilde{\Theta}$, desired system dynamics x_d are treated as variables and modeled as follows. The time derivative of the desired inductor current equation (\dot{x}_{1d}) can

be derived by taking the time derivative of the definition of x_{1d} , which is $x_{1d} = V_d^2 \hat{\theta} / \hat{E}$.

$$\dot{x}_{1d} = \left(\frac{V_d}{\hat{E}} \right)^2 (-\Gamma_1 \hat{\theta} \tilde{x}_1 - \Gamma_2 \hat{E} \tilde{x}_2 x_{2d}) \quad (10)$$

The control input u which follows from $\Psi = y \tilde{\Theta}$ can be expressed as,

$$u = 1 + \frac{1}{x_{2d}} (L \dot{x}_{1d} - \hat{E} - \mathcal{R}_1 \tilde{x}_1) \quad (11)$$

Substituting this control input back in $\Psi = y \tilde{\Theta}$, the dynamics of x_{2d} can be derived as,

$$\dot{x}_{2d} = \frac{1}{C} [(1-u)x_{1d} - \hat{\theta} x_{2d}] \quad (12)$$

Block diagram description of the complete system is shown in Fig. 2. The adaptation law block takes the two system state information (x), desired output voltage (V_d) and dynamically computed desired voltage (x_{2d}) to compute the estimates of the unknown parameter vector ($\hat{\theta}$) according to the relationship (9). The controller dynamics block utilizes system states, estimated parameter vector and desired output voltage to generate the control input to the plant (u) and dynamically computes the desired output voltage (x_{2d}) according to (11)-(12).

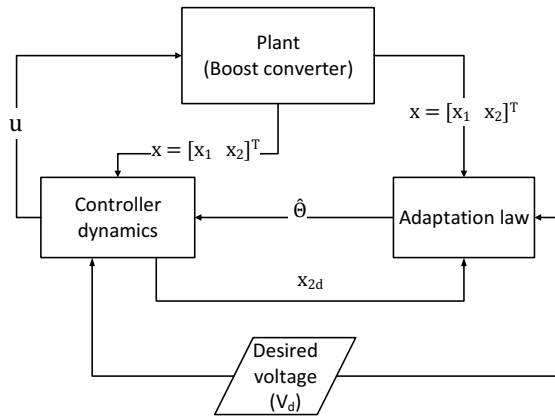


Fig. 2. Block Diagram of the complete system.

III. SIMULATION RESULTS

The simulations were carried out considering the boost converter parameters $L = 10 \text{ mH}$, $C = 500 \text{ } \mu\text{F}$, $E = 15 \text{ V}$, $R_o = 50 \text{ } \Omega$, $V_d = 30 \text{ V}$, $\mathcal{R}_1 = 0.2$, $\Gamma = I_{2 \times 2}$ and $\sigma = 0.05$. Three test cases were simulated to observe the state variations during startup, under desired output voltage change and subjected to a load change. Corresponding results are shown in Fig. 3 to Fig. 5.

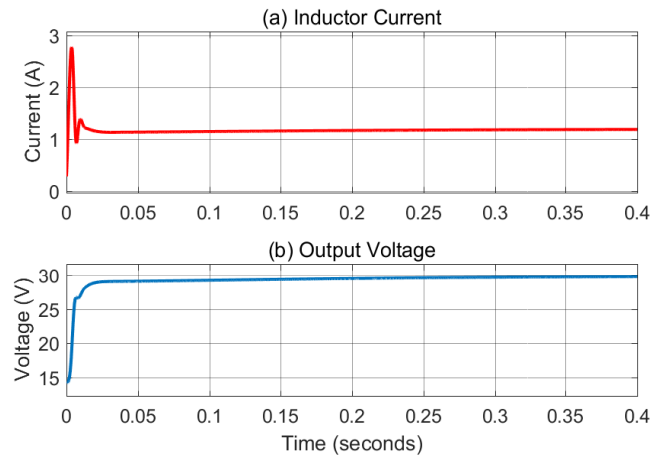


Fig. 3. Startup transient. (a) Inductor current and (b) Output voltage.

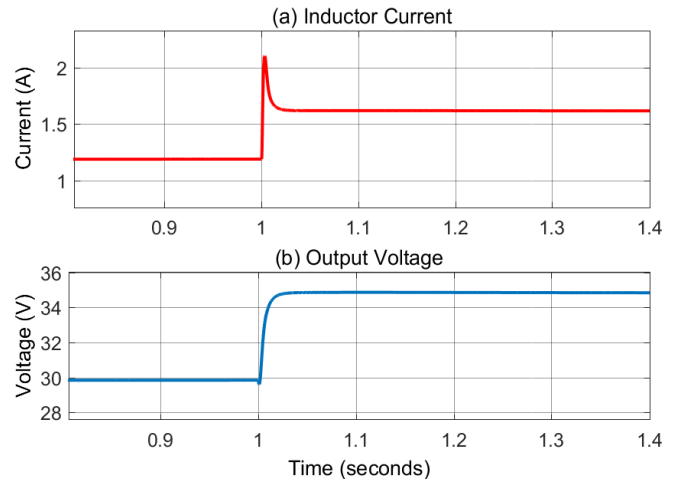


Fig. 4. Desired output voltage change. (a) Inductor current and (b) Output voltage.

A. Startup transient

Control system was initiated with no load initial conditions and variation of the system states were observed in this test case. According to the results shown in Fig. 3, output voltage reaches to the desired value of 30 V after 0.3 s . No overshoots are observed in the output voltage trajectory. However, there is an overshoot in the inductor current. The peak inductor current can be observed as 2.76 A and its steady state value is 1.18 A .

B. Desired output voltage change

Performance of the adaptive controller against a desired voltage change was explored in this simulation. The desired voltage was changed from 30 V to 35 V at $t = 1 \text{ s}$ and results are shown in Fig. 4. From the results it can be seen that both the output voltage and inductor current gain their respective new equilibrium within very short period of time of 30 ms . Output voltage reaches to 35 V without any overshoot or undershoot. Corresponding steady state inductor current is

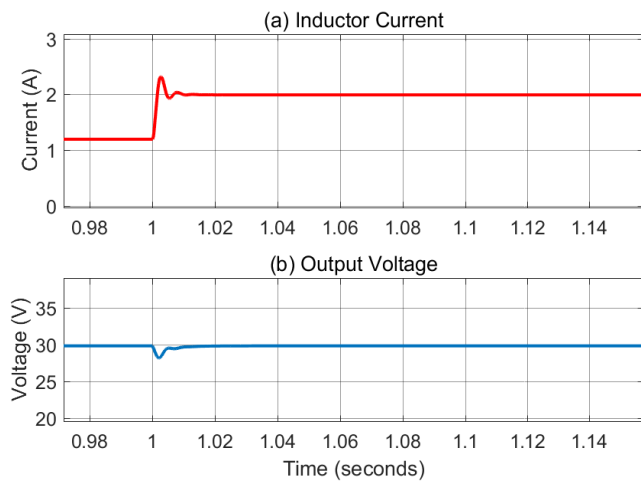


Fig. 5. Load change. (a) Inductor current and (b) Output voltage.

1.62 A. Further, a 2.1 A of peak can be observed in the inductor current during the transient period.

C. Load change

Adaptability and voltage regulation of the proposed controller under a load change was tested in this section. A step load change from $R_o = 50 \Omega$ to $R_o = 30 \Omega$ was given at $t = 1 s$. Obtained simulation results are depicted in Fig. 5. According to the results, it can be observed that the controller perfectly regulate the output voltage to the desired value even under the load disturbance. Variation in the voltage from its desired value at the point of load change is 1.8 V. After the load change, output voltage regains its desired value of 30 V less than 15 ms. Inductor current reach to its new steady state value of 1.98 A. An overshoot exists and the peak inductor current can be observed as 2.3 A.

IV. EXPERIMENTAL VALIDATION

Performance of the proposed controller was experimentally analyzed and results are given in this section. The controller and the converter were implemented based on MATLAB/Simulink and dSPACE control systems. Fig. 6 shows the experimental setup that contains DS1104 controller card, CP1104 I/O board, and MOSFET converter system. Switching frequency of the converter was set to 60 kHz. Corresponding experimental results of the three test cases simulated in the previous section are shown in Fig. 7 to Fig. 9. All the experimental results are closely match with the corresponding simulations.

Converter startup transient experimental results are given in Fig. 7 with 300 mA, 15 V initial conditions. As shown in Fig. 7, both inductor current and output voltage reach their steady state desired values within 0.4 s. Output voltage is regulated to 30 V and the inductor current during the steady state is 1.3 A. There are no overshoot or undershoot in the output voltage. However, an overshoot can be observed in the inductor current and its peak value is 1.8 A.

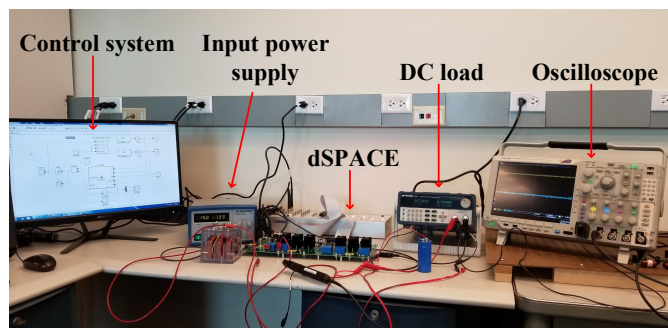


Fig. 6. Experimental test setup

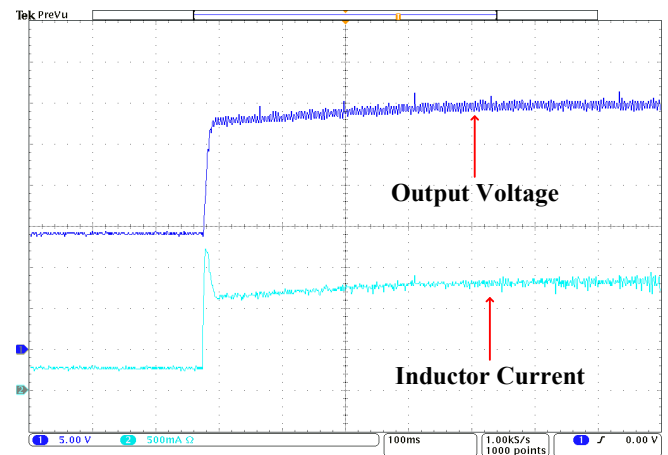


Fig. 7. Startup transient experiment.

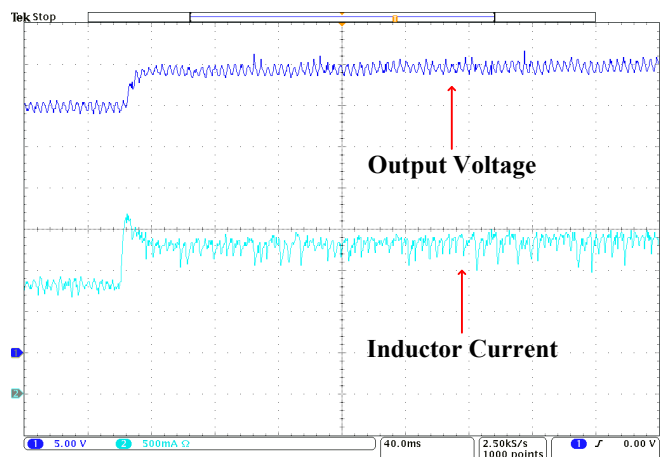


Fig. 8. Desired output voltage change experiment.

Variation of the experimental output voltage and inductor current subjected to a desired output voltage change is depicted in Fig. 8. Desired output voltage of the converter was changed from 30 V to 35 V. Both the system states reach their new equilibrium within very short period of time of 40 ms. New steady state output voltage is 35 V and inductor current

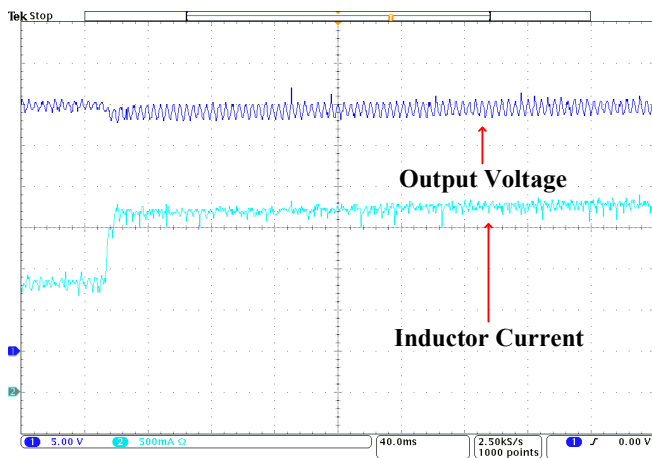


Fig. 9. Load change experiment.

is 1.8 A. No overshoot or undershoot is observed in the output voltage. However, peak inductor current at the point of disturbance is 2.2 A.

Controller performance under a load disturbance was experimentally validated by giving a step load change from $R_o = 50 \Omega$ to $R_o = 30 \Omega$ as in the simulation. Variation in output voltage and inductor current are illustrated in Fig. 9. As seen from the results, inductor current gains the new steady state at 2.2 A within very short time. There are no overshoots or undershoots are observed in either inductor current or output voltage. Due to the loading, slight voltage drop can be observed in the output voltage and it is less than 1 V.

V. CONCLUSION

Design of a passivity based adaptive controller to regulate the output voltage of a power electronic converter has been carried out in this paper. In contrast to most of the existing adaptive controllers, the proposed controller does not require the exact knowledge of either input voltage or output load resistance. Boost power converter has been used to develop the adaptive controller in this digest which can be extended to control any other DC-DC converter without loss of generality. Simulation and experimental results are given to illustrate the effectiveness and the applicability of the proposed approach. Both results show excellent voltage regulation during startup, under a desired voltage change and under a load disturbance. Extension of the proposed concept to multiple coupled power electronic converter system would be a possible future direction of this work.

REFERENCES

- [1] A. M. Dissanayake and N. C. Ekneligoda, "Transient optimization of parallel connected inverters in islanded ac microgrids," *IEEE Trans. Smart Grid.*, 2018, early access.
- [2] M. Pahlevaninezhad, P. Das, J. Drobnik, G. Moschopoulos, P. K. Jain, and A. Bakhshai, "A nonlinear optimal control approach based on the control-lyapunov function for an ac/dc converter used in electric vehicles," *IEEE Trans. Ind. Informat.*, vol. 8, no. 3, pp. 596–614, Aug 2012.

- [3] N. C. Ekneligoda and W. W. Weaver, "A game theoretic bus selection method for loads in multibus dc power systems," *IEEE Trans. Ind. Electron.*, vol. 61, no. 4, pp. 1669–1678, April 2014.
- [4] F. T. Asal and M. COŞGUN, "Pi, pd, pid controllers," *Middle East Technical University Electrical & Electronics Engineering*.
- [5] C. Chan, "A nonlinear control for dc-dc power converters," *IEEE Trans. Power Electron.*, vol. 22, no. 1, pp. 216–222, Jan 2007.
- [6] M. Salimi and S. Siami, "Closed-loop control of dc-dc buck converters based on exact feedback linearization," in *2015 4th International Conference on Electric Power and Energy Conversion Systems (EPECS)*, Nov 2015, pp. 1–4.
- [7] A. Maknouninejad, Z. Qu, F. L. Lewis, and A. Davoudi, "Optimal, nonlinear, and distributed designs of droop controls for dc microgrids," *IEEE Trans. Smart Grid.*, vol. 5, no. 5, pp. 2508–2516, Sept 2014.
- [8] N. C. Ekneligoda and W. W. Weaver, "Game-theoretic cold-start transient optimization in dc microgrids," *IEEE Trans. Ind. Electron.*, vol. 61, no. 12, pp. 6681–6690, 2014.
- [9] A. M. Dissanayake and N. C. Ekneligoda, "Online game theoretic feedback control of dc microgrids," in *2018 IEEE Power Energy Society Innovative Smart Grid Technologies Conference (ISGT)*, Feb 2018, pp. 1–5.
- [10] J. Wang, C. Zhang, S. Li, J. Yang, and Q. Li, "Finite-time output feedback control for pwm-based dc-dc buck power converters of current sensorless mode," *IEEE Trans. Control Syst. Technol.*, vol. 25, no. 4, pp. 1359–1371, July 2017.
- [11] H. J. Sira-Ramirez and R. Silva-Ortigoza, *Control design techniques in power electronics devices*. Springer Science & Business Media, 2006.
- [12] P. A. Ioannou and J. Sun, *Robust adaptive control*. PTR Prentice-Hall Upper Saddle River, NJ, 1996, vol. 1.
- [13] S. Kazemlou and S. Mehraeen, "Decentralized discrete-time adaptive neural network control of interconnected dc distribution system," *IEEE Trans. Smart Grid.*, vol. 5, no. 5, pp. 2496–2507, 2014.
- [14] T. K. Nizami and C. Mahanta, "An intelligent adaptive control of dc-dc buck converters," *Journal of the Franklin Institute*, vol. 353, no. 12, pp. 2588–2613, 2016.
- [15] Y. Cheng, H. Du, C. Yang, Z. Wang, J. Wang, and Y. He, "Fast adaptive finite-time voltage regulation control algorithm for buck converter system," *IEEE Trans. Circuits Syst. II*, vol. 64, no. 9, pp. 1082–1086, 2017.
- [16] H. Sira-Ramirez, R. Ortega, and M. García-Esteban, "Adaptive passivity-based control of average dc-to-dc power converter models," *International journal of adaptive control and signal processing*, vol. 12, no. 1, pp. 63–80, 1998.
- [17] S. Oucheriah and L. Guo, "Pwm-based adaptive sliding-mode control for boost dc-dc converters," *IEEE Trans. Ind. Electron.*, vol. 60, no. 8, pp. 3291–3294, 2013.
- [18] Y. Bao, L. Y. Wang, C. Wang, J. Jiang, C. Jiang, and C. Duan, "Adaptive feedforward compensation for voltage source disturbance rejection in dc-dc converters," *IEEE Trans. Control Syst. Technol.*, vol. 26, no. 1, pp. 344–351, 2018.
- [19] R.-J. Wai, L.-C. Shih *et al.*, "Adaptive fuzzy-neural-network design for voltage tracking control of a dc-dc boost converter," *IEEE Trans. Power Electron.*, vol. 27, no. 4, pp. 2104–2115, 2012.
- [20] P. T. Krein, *Elements of power electronics*. Oxford University Press New York, 1998, vol. 126.